Petroleum Res. J. Vol. 18 (2005); P. 51-58, 11 Figs.

2-D Geological Modeling in the Vicinity of Horizontal Wells – Case Study Integrating Borehole Images and Openhole logs

Aimen Amer*

نمذجة جيولوجية ثنائية الأبعاد بجوار آبار أفقية - دراسة حالة دمج صور وسرود البئر

أيمن عامر

معلومات ميل الطبقات المستنبطة من جهاز قياس ميل الطبقات ومعدات التصوير لا يتم عادة دمجها مع سرود البئر، وبالتالي فإن العلاقة بينهما سؤال يجب الإجابة عليه. ستوضح هذه الورقة أساليب جديدة لاستحداث نمذجة جيولوجية ثنائية الأبعاد ترتكز أساسا على صور سرود البئر ووصفه، وذلك باستخدام مثال حقلي في آبار أفقية.

تزود تفسيرات صور السرود والعينات بمعلومات قيّمة عند جدار البئر وبالإمكان إسقاطها على المنطقة المجاورة له عن طريق إنشاء قطاع تركيبي باستخدام الحاسوب (شكل تركيبي). إن الصورة الحالية للشكل التركيبي مخصصة إلى معلومات الميل ولا يمكن دمج معلومات سرود الآبار في القطاع التركيبي المعد ومع ذلك فإن وصف البئر يمكن دمجه في القطاع التركيبي عن طريق أجزاء من السحنات الصخرية المتحصل عليها من السرود على طول حدود الطبقة المتعرف عليها مسبقا بالقطاع التركيبي باستخدام برمجة الحاسوب.

إن النموذج العام لا يعكس دائما البنية الحقيقية المحيطة بالبئر وهذا بالطبع يعتمد على اتجاه المقطع باعتباره غير عمودي على بنية التكاوين الجيولوجية. ولقد بين تفسير الدراسة السيزمية ثنائية الأبعاد، من دراسة الحالة للبئر الأفقي، وجود منخسفات ومرتفعات، وأن هذا النظام البنيوي يتجه ناحية شمال شرق – جنوب غرب فقط. ورغم ذلك فإن المعلومات السيزمية ثلاثية الأبعاد قد تم جمعها أثناء عملية وصف العينات.

تم حفر قطاع أفقي يصل إلى 1820 قدم بواسطة "LWD-"GR، ووجد أن هذا المقطع الأفقي الطويل نسبيا قد اخترق 260 قدما من صخور سميكة من الطفلة الجيرية المانعة لهجرة النفط تلته صخور جيرية تشكل صخور المكمن.

ومن أجل حل مشكلة الحفر عبر طبقة صخور الطفلة الجيرية وتفهّم بنية وجيولوجية صخور المكمن تم الحصول على (صور وسرود الآبار).

يوضح النموذج الناتج أن للبئر ست نطاقات بنيوية مختلفة وبه سبعة صدوع معكوسة وتحت سيزمية، كما بين هذا النموذج مصيدة بنيوية للتطوير المستقبلي. وبعد الانتهاء من وضع النموذج ثنائي الأبعاد أوضح النموذج السيزمي ثلاثي الأبعاد وجود صدوع عكسية بالإضافة إلى المصيدة التركيبية.

لقد بينت دراسة الحالة هذه أن إنتاج النموذج الجيولوجي ثنائي الأبعاد ضروري لتقدير دقيق للوضع البنيوي والجيولوجي للبئر خاصة خلال المراحل الأولى من الاستكشاف وعندما تكون المعلومات محددة وغير مؤكدة ولا يقتصر تطبيق هذه الطريقة المطورة والمطبقة في هذه الورقة على الآبار الأفقية بل يمكن تطبيقها على الآبار العمودية والمائلة.

Abstract: *Dip data obtained from dipmeters and imaging tools are not usually integrated with openhole logs. This paper addresses the relationship between these two types of data and uses a horizontal well to illustrate a new methodology that produces a two-dimensional (2-*

* Schlumberger Overseas, Oman.

D) geological model based on borehole images and openhole logs.

Images provide valuable information about the borehole wall and can be easily extended to the borehole vicinity by using softwares to construct a structural cross-section. Although the software used in this study is devoted for dip data and cannot integrate openhole logs into the constructed cross-section, the log data were integrated by populating the lithofacies obtained from the logs along the bed boundaries previously identified using other software programs.

The generated model did not always reflect the true structures surrounding the well. Accuracy depended on the direction of the cross-section, and the section was not always perpendicular to the structure. However, computing and displaying the different structural zones resolved this issue.

In the case study, 2-D seismic data showed a graben and horst system with only one structural trend, oriented NE-SW. Three-dimensional (3-D) seismic data were being processed at the time of logging and were used later to validate the model. During drilling of the 1,820-ft horizontal section, which included 260 ft of cap rock, a logging-while-drilling (LWD) gamma ray log was obtained. The Cretaceous carbonate reservoir section was directly beneath the cap rock, which was composed of a thick layer of calcareous shales.

To resolve the issue of drilling through the calcareous shales and to understand the structure and geology of the reservoir, borehole images and openhole logs were acquired.

The model constructed from the images and logs identified six different structural zones (including a fold) and seven reverse faults. It also defined a structural trap with potential for further development. The newly processed 3-D seismic survey showed four reverse faults in addition to the trap, confirming the 2-D model.

This case study illustrates that a 2-D geological model is critical for accurate structural and geological definition of the wellbore environment, especially during the early exploration stages when data are limited and uncertainties are high. The procedures developed and applied in this paper are not restricted to horizontal wells; they can also be applied to vertical and deviated wells.

INTRODUCTION

High-resolution imaging tools deliver huge amounts of data, and much of this data is not convenient to use or is not fully used. The main goal of this paper is to illustrate a methodology to summarize borehole image data and lithological evaluation derived from openhole logs in one geological model (cross-section). In analogy with problems in structural geology, one might first think of cross-sections in terms of assessing a geological model (Anxionnaz and Delhomme, 1998).

The model in this article is presented as a workbench on which to refine and interpret all available well data. Nevertheless, producing such a model from raw dip data provides the geologist with insights for reservoir analysis, especially during early field appraisal. An example of these insights is illustrated in Figure 1 and leads to a better understanding of the reservoir structure.

From a geological point of view, two types of information can be used to define the reservoir geometry: seismic data and borehole images/logs. The resolution of seismic data is improving, but if structures are too small (less than 50 m), the average dip is too high, or the velocity contrast is too low, significant structures may be missed on seismic sections. In each of these cases, seismic techniques are insufficient to achieve an accurate structural description of the reservoir (Etchecopar and Bonnetain, 1992). Meanwhile, geologists, petrophysicists, and geophysicists use borehole images, dipmeters and log data in a wide range of applications to reduce the uncertainties.

The model in this paper follows the technique of Etchecopar and Bonnetain (1992), in which they introduced a computer method to produce structural cross-sections from dipmeter and imaging data. The

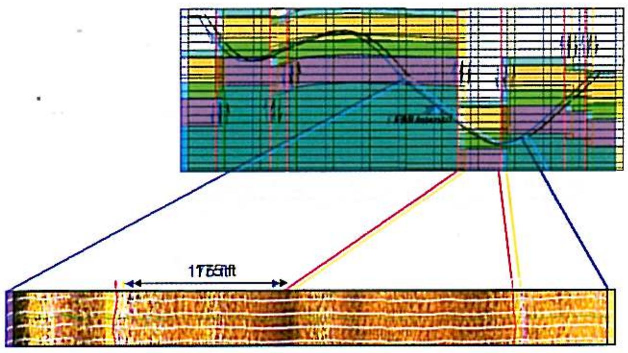

Fig. 1. The faults on this model were interpreted before acquisition of borehole images. The images confirm the fault but clearly show a 175-ft offset from one of the previous (seismic) interpretation.

constructed cross-section is based on a similar fold model (Ramsay, 1967) used to describe folds, faults, and even rollovers.

The interpretation of dipmeter data is not new. Authors such as Busk (1929), Gilreath and Maricelli (1964), Vincent *et al.* (1979), and Suppe (1985) have proposed methods to extract the information by pattern recognition. Others, such as Bengston (1981), proposed new projection methods to make the interpretation of dipmeter results easier.

Although the referenced techniques have greatly improved the structural and geological interpretation of dip data, they do not address the main goal of the geologist, which is integrating all openhole log data into one model in a short time frame.

METHODOLOGY

Our modeling is based on the technique introduced by Etchecopar and Bonnetain (1992), who based their method on two fundamental behaviors of strata during deformation: similar folding and parallel folding. There is a main constraint on the produced model, where they have to be strictly consistent with the dips measured in the well. Even with this constraint, it is often possible to interpret a single dataset as a fold or as a fault, with consistent results in both cases. The final decision about which type of structure is to be used, depends on regional knowledge.

The technique has now evolved into a software that converts a bunch of loose tadpoles into a meaningful structural cross-section. Because of its applicability to different types of structures, it is based on two hypotheses: similarity and cylindricity. These hypotheses imply that the position in space of layer boundaries can be derived from each other by a simple translation along a translation plane.

The current version of the software is devoted to dip data and cannot integrate openhole logs into the constructed cross-section. However, the openhole logs can be integrated into the structural cross-section by populating the lithofacies obtained from the logs along the software-identified bed boundaries using other computer methods (Figs. 2 and 3).

(1) (2)

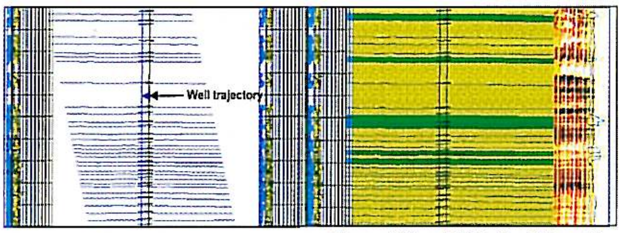

The output result of the computer program using a simple fold model.

The population of bed boundaries and lithological data along the predefined bed boundaries based on borehole images and openhole logs, while integrating with the structural cross-section.

Fig. 2. Steps leading to a 2-D geological model in a vertical well.

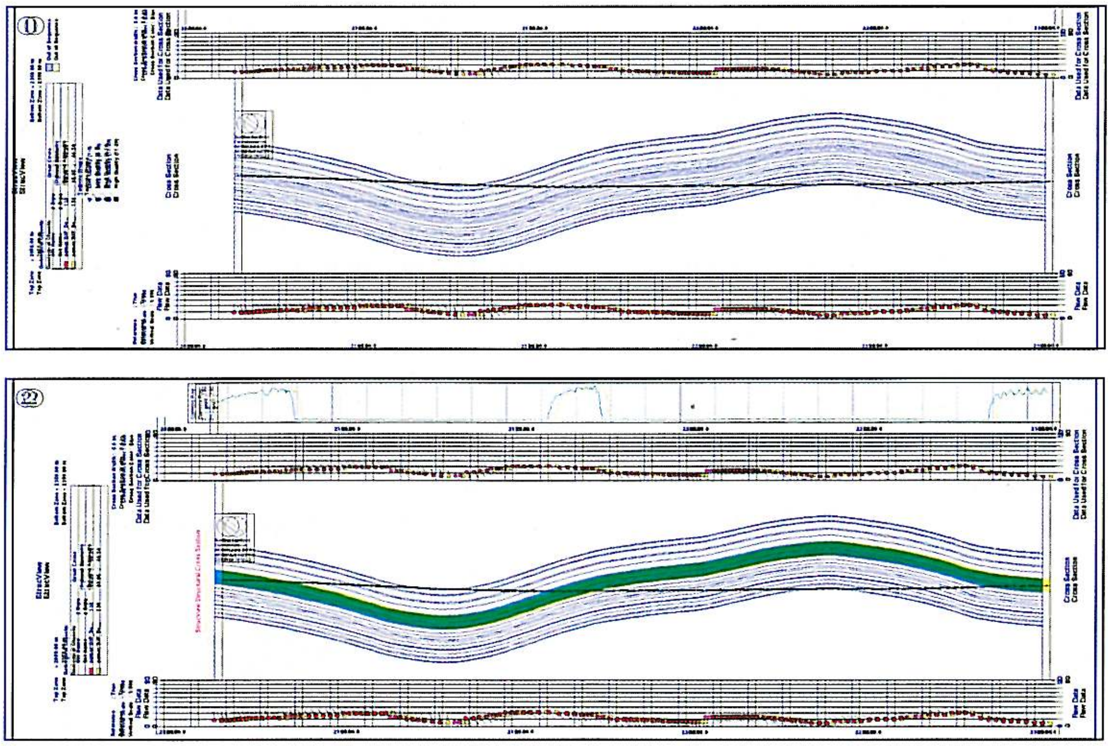

Fig. 3. A simple horizontal well structural model. (1) The output result of the computer program. (2) Using other computer programs we can populate the lithological data on the basis of openhole gamma ray log.

The field example presented in this paper has two types of input data: dips (beddings and faults) obtained from the imaging data (structural model) and the openhole logs (lithology). These two inputs are used simultaneously in a computer method to generate a 2-D geological model, which shows the structural and geological setting of the well.

The ability of the generated model to reflect true structural dip depends on the orientation of the cross-section and the complexity of the structure, because the model is not always perpendicular to the structure. To avoid this situation, different structural zones are computed and plotted beside the cross-section to reflect the real structural dip magnitude and azimuth direction in conjunction with the well trajectory.

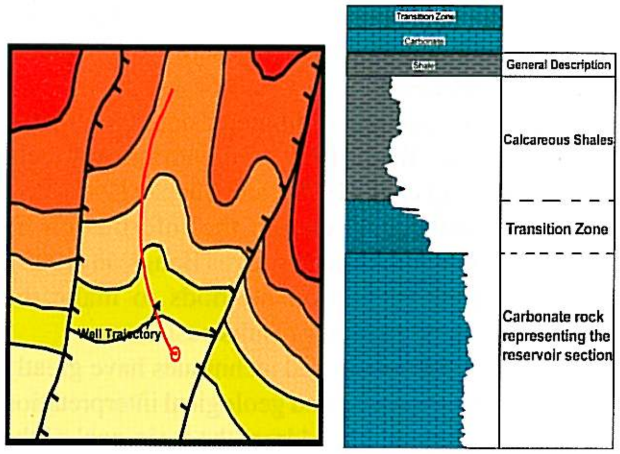

Fig. 4. Schematic drawing of the structural setting of the well before modeling and the stratigraphic summary of the drilled section.

HORIZONTAL WELL CASE STUDY

The number of horizontal wells is increasing, and identifying the geological and structural characterization of the reservoirs targeted by these wells is critical, because of the drastic lateral and vertical changes that occur both in facies or structure. It was not so long ago that reservoir studies were based mainly on cores, openhole logs, outcrop measurements, and, most importantly, seismic data.

Seismic surveys give accurate information in low and simple dip zones, whereas imaging data are more useful in identifying highly variable, steeply dipping zones and viewing sub-seismic features. However, local experience demonstrates that many important structural features cannot be interpreted from seismic data, especially at great depths.

In this case study, 2-D seismic data, interpreted prior to drilling the well, showed a graben and horst system, and no faults were interpreted along the well trajectory (Fig. 4). The structural system, as illustrated, trends to the NE-SW, and there are no other structural trends. During drilling of the 1,820-ft horizontal section, which included 260 ft of the cap rock, a gamma ray log was recorded. After drilling through the cap rock, composed of a thick layer of calcareous shales, the Cretaceous carbonate reservoir section was reached for the second time (Fig. 4).

Borehole imaging data and openhole logs were acquired to resolve the issue of drilling through the calcareous shales and to understand the structure and geology of the reservoir.

BOREHOLE IMAGE INTERPRETATION

The goal of image interpretation is to characterize formation properties. This information assists geologists in their studies and assists petroleum engineers in determining permeability paths and barriers, calculating net pay, and planning of well completions such as perforations and hydraulic fracturing. The interpretation itself is a multi-step process of observation, description, interpretation, and implementation or exploitation (Serra, 1989).

There are different types of imaging tools, and the principle of measurement changes from one tool to the other. The two main types of measurements are resistivity and acoustic (Fig. 5). The imaging tool used in this case study is an acoustic imaging tool. Acoustic images do not normally give sufficient resolution for detailed sedimentological studies, because they are very sensitive to borehole conditions (Hansen and Fett, 2000). However, in this case the

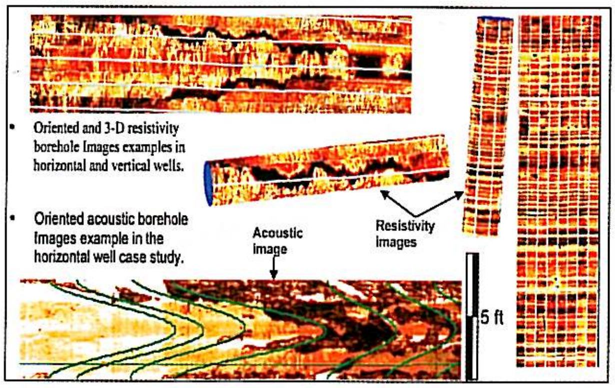

Fig. 5. Resistivity and acoustic images, horizontal and vertical, showing bedding planes.

images fulfill the objective, which is identifying the structural and geological setting of the well.

The high-quality image obtained allowed confident interpretation of bedding, fractures, borehole breakouts, faults, and vugs. Fractures and bedding dips are defined, shown as low- and high-amplitude sinusoidal patterns, respectively. Borehole breakouts are also recognized, seen as axial low-amplitude (dark) bands running along the axis of the image. Vugs are seen as dark spots, randomly distributed or sometimes aligned with bedding planes, with variable shape and size. The fault interpretation is based on the observed termination of bedding planes against the fault plane. This interpretation also includes the sharp changes in the image texture across the fault planes. Seven faults were interpreted on the acoustic images; no faults were interpreted previously from seismic data (Fig. 6). The structural dip is computed using the local curvature technique (Etchecopar and Dubas, 1992).

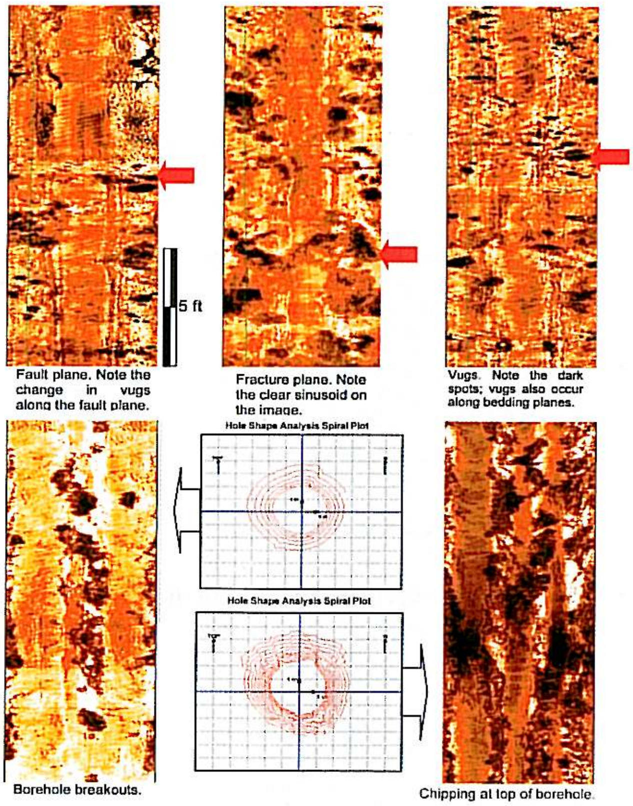

Fig. 6. Acoustic image examples along the horizontal section. All images are oriented top of hole. (After Amer and Abushaala, 2002).

This technique allows the user to subdivide the study interval into different structural zones or sub zones based on major changes in the structural dip magnitude and/or azimuth (Fig. 7). The bedding azimuthal vector plot shows the intra-formation variations of bedding orientation in the uphole

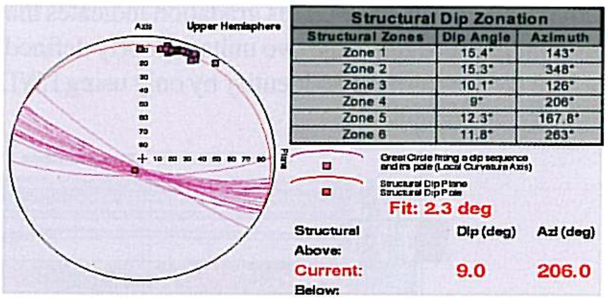

Fig. 7. Structural zonation and a Schmidt plot illustrating the local curvature axis computed over Zone 4.

direction. The bedding azimuth on the vector plot shows SW, S, and SE azimuthal trends (arc shape). These directions coincide oppositely with the well azimuth, indicating the well was drilled in the up dip direction for most of the section (Fig. 8). This up dip drilling is also observed on the geological cross-section, which is discussed in the following section. The vector plot also shows a zone of disturbance where the azimuths are changing drastically. This change outlines a fold, which is confirmed by the acoustic image and the structural dip zonation. These changes in the vector plot are due to the fact that we moved through the axis of the fold, from one limb of the fold to the other.

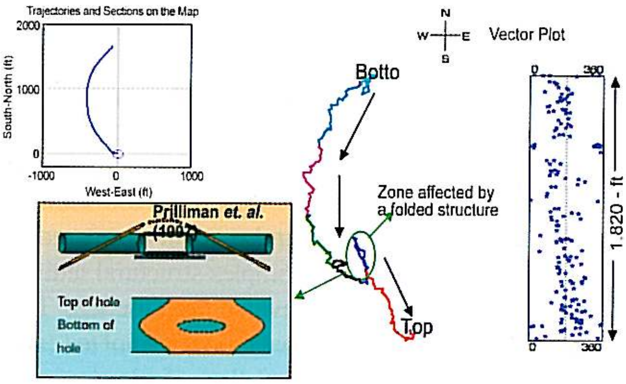

Fig. 8. Well trajectory map view and total bedding vector plot, showing the relationship between the drilling direction and beddings.

2-D MODELING

The integration of borehole images with all other available formation evaluation data is critical for accurate structural and geological assessment, especially during early exploration stages. The integration of this dataset clearly illustrates that the first entry of the well trajectory into the calcareous shales is marked by a vertical gradational change in lithology (Figs. 4 and 9). This gradation indicates that the contact between these two units is poorly defined, which made it difficult to identify by only using LWD gamma ray data. This transition zone is marked on the ultrasonic images (Fig. 10). The presence of ENE-WSW trending fault resulted in the well trajectory

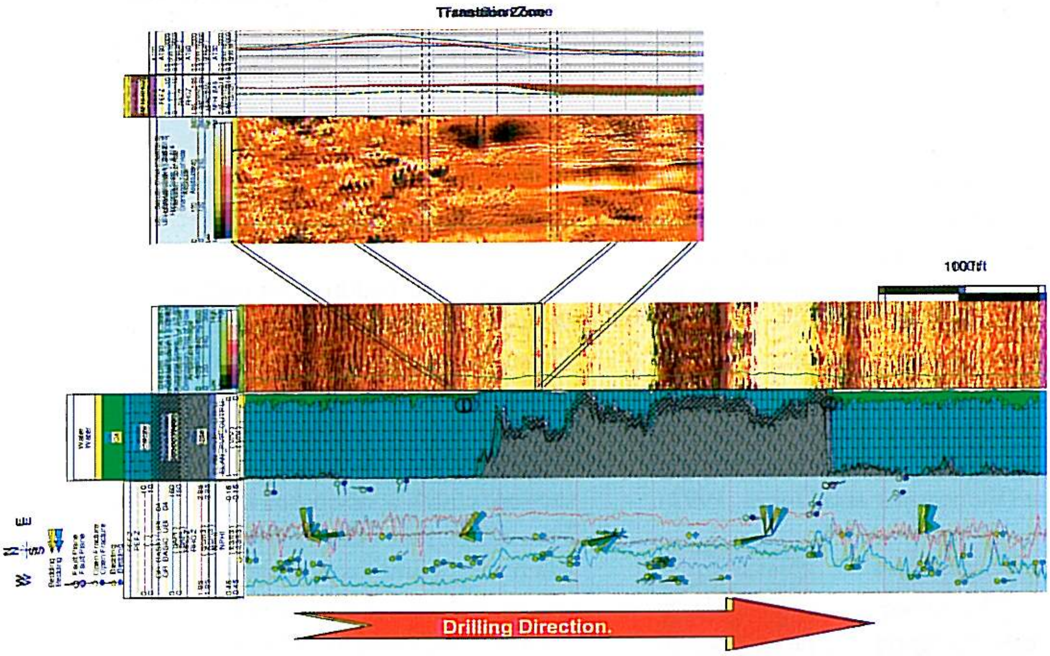

Fig. 9. A part of the well interval that crosses the cap rock. Note the smooth transition in the shale content at Point (1) resulting from the gradational change in facies and the sharp break at Point (2) caused by a fault.

reentering the reservoir zone for a second time. This reentry is very clear on both the acoustic image and openhole logs (Fig. 10).

After analyzing both the borehole images and openhole logs, the cross-section can be computed along a SE-NW, S-N, and a SW-NE line to fit the arc-shaped well trajectory. During cross-section generation, different structural models were used to determine the best fit to the complex structural setting: monocline, anticline, and reverse fault models. The fault displacements on the final model are not to scale, and the relative movement of these faults (reverse movement) are based only on the relationship between the borehole images and openhole logs.

The reverse faulting was unexpected, because this field is known to have a normal fault system. An interpretation of the processed 3-D seismic data confirmed the model with four reverse faults and a structural trap between Zones 3 and 4 (Fig. 10).

The structural dip computed using the local curvature axis technique was plotted beside the cross-section to give the true structural picture. The display revealed a domal structure (fold), a NE-SW striking axis between the two structural zones, Zones 1 and 2. Although this fold is not

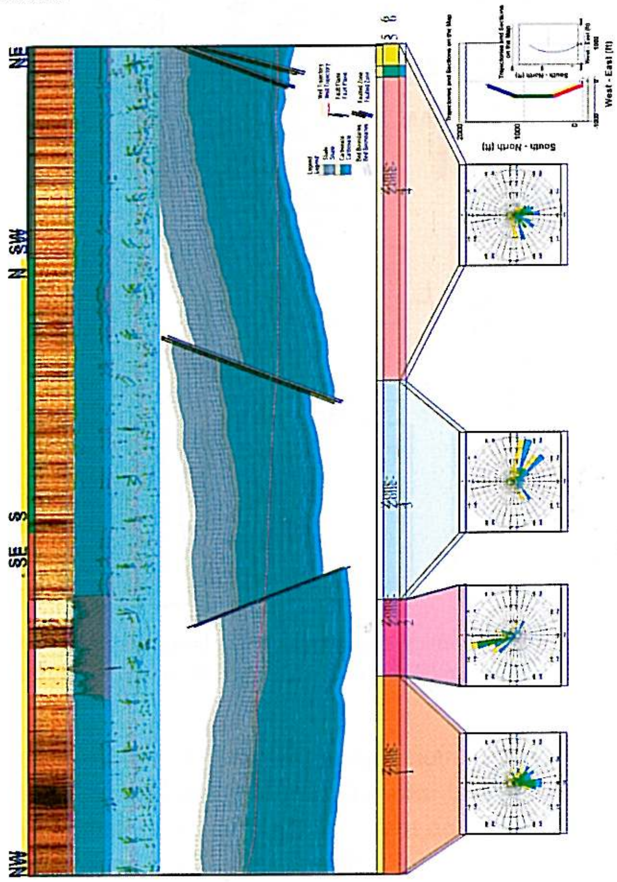

Fig. 10. 2-D geological model and structural zonation and azimuthal plots. The map view shows the direction of the cross-section.

observed on the model because the cross-section direction is not perpendicular to the structure, it is clear from the structural zones, bedding azimuth, and vector plots.

DISCUSSION

The high-quality acoustic image allowed confident interpretation of different geological features (e.g., bedding, fractures, borehole breakouts, faults, and vugs). These interpreted structural and/or sedimentological features added value to the reservoir characterization and increased the resolution of the geological, petrophysical, and seismic models.

The interpreted bed boundaries and fault planes gave a clear picture of the well's surrounding structure and fault systems (Fig. 10). The fractures and vugs were used to calculate the secondary porosity, which has a direct impact on production. The breakouts and borehole chipping analysis will be used to alleviate or avoid future drilling problems (Fig. 6). The fault identification has been used to update the available seismic maps and increase their resolution and accuracy (Fig. 11).

Before After

Fig. 11. Schematic drawing of the structural setting of the well before and after updating the map with the modeling data.

CONCLUSIONS

The 2-D geological model, based essentially on borehole images, illustrated a high degree of resolution when the images were integrated with available openhole log data.

The bedding analysis subdivided the logged interval into six structural zones. These zones mark the major changes within the structural dips and include a fold with a NE-SW striking axis. The interpretation also revealed seven reverse faults, and indicates that drilling was in the up dip direction.

The 2-D geological model, which has the same 0.2-in. resolution as the imaging tools, shows a great level of detail and accuracy. The production of such a model from dip data computed from borehole images provides the geologist with insights for reservoir analysis, especially during early field appraisal, when data are limited and uncertainties are high. In addition, this model can be integrated with seismic data for static modeling purposes. The technique is not restricted to horizontal wells; it can also be applied to vertical and deviated wells.

REFERENCES

[1] Amer A. and Abushaala S., 2002. *Fullbore Formation MicroImager and ELAN* Processing and Interpretation*, (Schlumberger internal report).

[2] Anxionnaz, H. and Delhomme, J.P., 1998. Near-wellbore 3-D reconstruction of sedimentary bodies from borehole electrical images. SPWLA Annual Logging Symposium.

[3] Bengston, C. A., 1981. Statistical curvature analysis techniques for structural interpretation of dipmeter data. *Bul. Am. Assoc. Petrol. Geol.*, ***65***, 2, 312-332.

[4] Busk, H.G., 1929. *Earth Flexures*. Cambridge University Press, p. 106.

[5] Etchecopar, A. and Bonnetain, J.L., 1992. Cross-sections from dipmeter data. *Bul. Am. Assoc. Petrol. Geol.*, **76**, 5, 621-637.

[6] Etchecopar, A. and Dubas, M.O., 1992. Methods for geological interpretation of dips. SPWLA Annual Logging Symposium proceedings, Paper J.

[7] Gilreath J. A. and Maricelli, J.J., 1964. Detailed statigraphic control through dip computation. *Bul. Am. Assoc. Petrol. Geol.*, **48**, 12, 1902-1910.

[8] Hansen, S.M and Fett, T., 2000. Identification and evaluation of turbidite and other deepwater sands using open hole logs and borehole images, *in* A.H.

[9] Prilliman, Jeff, Bratton, Tom, Fredette, Mark. A, Lovell, John R., Bean, Clarke L., and Hashem, Mohamed, 1997. A Comparison of Wireline and LWD Resistivity Images in the Gulf of Mexico. First published on the I^{2S}, November 1997.

[10] Ramsay, J. G., 1967. *Folding and Fracturing Rocks*. New York McGraw-Hill, 568 p.

[11] Serra, O., 1989. *Formation MicroScanner Image Interpretation*. Schlumberger Educational Services, Houston, Texas.

[12] Vincent, P., Gartner J., and Attali, G., 1979. GEODIP—an approach to detailed dip determination using correlation by pattern recognition. *J.Petro. Tech.*, **31**, 232-240.